

Electronic structure of $RAuSn$ ($R=Sc, Ce, Gd, Er$, and Lu) investigated with x-ray photoelectron spectroscopy and band structure calculations

Jan Gegner,¹ Hua Wu,¹ K. Berggold,¹ C. P. Sebastian,² T. Harmening,² R. Pöttgen,² and L. H. Tjeng¹

¹*II. Physikalisches Institut, Universität zu Köln, Zùlpicher Straße 77, D-50937 Köln, Germany*

²*Institut für Anorganische und Analytische Chemie, Westfälische Wilhelms-Universität Münster, Corrensstraße 30, D-48149 Münster, Germany*

(Received 10 October 2007; published 2 January 2008)

We have investigated the electronic structure of the intermetallic compounds $ScAuSn$, $CeAuSn$, $GdAuSn$, $ErAuSn$, and $LuAuSn$ using x-ray photoelectron spectroscopy and band structure calculations. We find good general agreement between the experimental and calculated valence band spectra, provided that the spin-orbit interaction in the Au bands as well as correlation effects in the open rare-earth $4f$ shell are included in the calculations. The rare-earth $4f$ and Au $5d$ have well identified spectral features far away from the Fermi level. The spectral weight in the vicinity of the Fermi level is built up of mainly Au/Sn sp and rare-earth spd bands. We find an extremely low or vanishing spectral weight at the Fermi level for $ScAuSn$ and $LuAuSn$, consistent with their semiconducting behavior as revealed by temperature dependent resistivity measurements.

DOI: 10.1103/PhysRevB.77.035103

PACS number(s): 71.20.Eh, 79.60.-i

The crystal chemistry and physical properties of the equi-atomic rare-earth (R) gold stannides $RAuSn$ have been subject to a large number of studies in the past 30 years.¹ They crystallize in two different structures, depending on the R sizes. For the larger rare earths ($R=La-Nd, Sm, Gd-Dy$) the hexagonal $NdPtSb$ type^{2,3} is adopted, which is a ternary ordered variant of the AlB_2 structure with two-dimensional networks of puckered Au-Sn hexagons (see Fig. 1). For the smaller R ($R=Sc, Tm$, and Lu), $RAuSn$ crystallize in the cubic $MgAgAs$ type⁴ or half-Heusler structure. In this structure, Au and Sn form a zinc blend substructure with the R ions filling the octahedral voids. For $R=Ho$ and Er , both types of structure can be adopted.⁵⁻⁸ The $RAuSn$ compounds with $R=Ce-Nd, Gd-Er$ order antiferromagnetically with Néel temperatures ranging from 2.8 K for $PrAuSn$ up to 35 K for $GdAuSn$.⁶⁻¹⁴

In view of the large number of investigations on this class of intermetallic materials, it is rather surprising that only few experimental¹⁴⁻¹⁷ efforts have been made to determine the electronic structure. We have therefore performed x-ray photoelectron spectroscopic measurements on $RAuSn$ for $R=Sc, Ce, Gd, Er$, and Lu , thereby encompassing the two different crystal structures as mentioned above. We also have calculated the band structure of these materials using the local density approximation (LDA) and local density approximation + Hubbard U (LDA+ U) scheme,¹⁸ where the U is used to account for correlation effects in an open atomic like $4f$ shell. It turned out that it was necessary to include the Au $5d$ spin-orbit coupling as well for obtaining good agreement with the observed valence band spectra. Special attention was paid to the density of states in the vicinity of the Fermi level and the predicted semiconducting character of the cubic compounds.^{19,20}

The starting rare-earth, noble metal, and tin materials were mixed in the ideal 1:1:1 atomic ratios and arc-melted as described previously.¹ The polycrystalline samples with dimensions of about $2 \times 2 \times 2$ mm³ are silvery with metallic luster and are stable in air over months. All samples were pure phases on the level of x-ray powder diffraction. The photoemission spectra were recorded at room temperature in

a spectrometer equipped with a Scienta SES-100 electron energy analyzer and a Vacuum Generators twin crystal monochromatized Al $K\alpha$ ($h\nu=1486.6$ eV) source. The overall energy resolution was set to 0.4 eV, as determined using the Fermi cut off of an Ag reference which was also taken as the zero of the binding energy scale. As an alternative and convenient energy reference, the Au $4f_{7/2}$ core level of polycrystalline Au metal at 84.00 eV binding energy was recorded before and after each measurement of the intermetallic samples. The base pressure in the spectrometer was 1×10^{-10} mbar, and the pressure raised to 2×10^{-10} mbar during the measurements due to the operation of the x-ray source. The samples were cleaved *in situ* to obtain clean surfaces.

The left panels of Fig. 2 show the experimental valence band photoemission spectra of the hexagonal compounds $CeAuSn$, $GdAuSn$, and $ErAuSn$ (from top to bottom) and the right panels those of the cubic compounds $ScAuSn$ and $LuAuSn$ (from top to bottom). The spectra of all compounds have in common that they show a doublet structure between 4 and 7 eV binding energies. Using the results from a previous study on the $RAuMg$ system,²¹ we can assign this doublet structure to the Au $5d$ levels, split up by the spin-orbit interaction. For $GdAuSn$, $ErAuSn$, and $LuAuSn$, the contribution of the rare-earth $4f$ orbitals is clearly visible. In $GdAuSn$, a broad peak appears at 8.8 eV binding energy, typical for the photoemission from the $4f^7$ configuration of Gd^{3+} . The width of the peak is much broader than the ex-

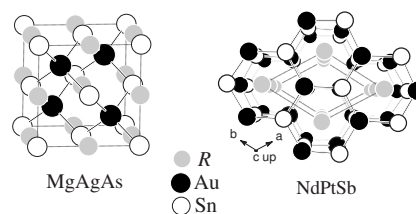


FIG. 1. Crystal structure of the intermetallic compounds $RAuSn$. On the left-hand side, the cubic $MgAgAs$ type and on the right-hand side, the hexagonal $NdPtSb$ type are drawn.

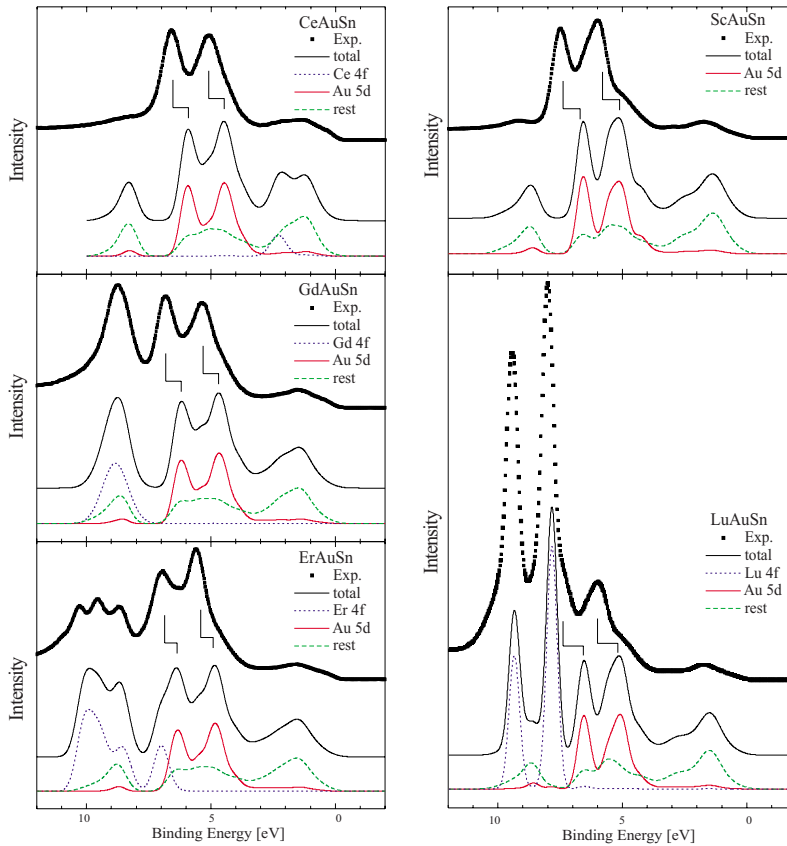


FIG. 2. (Color online) Experimental valence band photoemission spectra and calculated valence band density of states of the hexagonal compounds CeAuSn, GdAuSn, and ErAuSn (left panels) and of the cubic compounds ScAuSn and LuAuSn (right panels). A Gaussian broadening of 0.5–0.7 eV has been included in the calculated density of states.

perimental resolution and reflects the multiplet structure of the $4f^6$ final state.^{22–24} In ErAuSn, the triplet structure between 8 and 11 eV binding energies and some weight superposed on the Au 5d peak at 5.6 eV binding energy can be attributed to the photoemission from a $4f^{11}$ ground state of Er^{3+} leading to a $4f^{10}$ final state.^{22–24} In LuAuSn, the doublet structure at 8.1 and 9.5 eV binding energies is characteristic for the spin-orbit split $4f_{7/2}^{13}$ and $4f_{5/2}^{13}$ final states of Lu^{3+} with a $4f^{14}$ ground state.^{22–24} In CeAuSn, the 4f contribution (around 2 eV binding energy) is not as obvious as in the other compounds. For Ce, a $4f^1$ configuration is expected, resulting in much less spectral weight compared to the other rare earths with 7, 11, or 14 4f electrons since the total 4f spectral weight is roughly proportional to the number of 4f electrons.²⁵

To extract further information from the experimental spectra, we performed LDA and LDA+ U band structure calculations using the full-potential augmented plane waves plus local orbital method.²⁶ The crystal structures were taken from x-ray diffraction measurements.^{1,6,14,27} The muffin-tin sphere radii were chosen to be 3.2/2.5/2.5 bohr for Ce(Gd)/Au/Sn, and 2.7/2.5/2.5 bohr for Sc(Er,Lu)/Au/Sn. The choice of the larger Ce and Gd muffin-tin spheres is associated with the longer Ce(Gd)-Au and Ce(Gd)-Sn bond lengths in their layered structures. The cut-off energy of 16 Ry is set for the plane-wave expansion of the interstitial wave functions. 5000 (2500) \mathbf{k} points are used for integration over the Brillouin zone of the cubic (hexagonal) cell. Spin-orbit coupling of the valence electrons is included by the second-variational method with scalar

relativistic wave functions. The deep-level core electrons are treated fully relativistically.

The LDA/LDA+ U results are also shown in Fig. 2. One can observe that the calculations reproduce well the line shape of the Au 5d levels but underestimate systematically their binding energy by about 0.6–0.8 eV which is indicated by the angulated lines. This can be attributed to the inherent limitation of the mean-field method to describe excitation spectra. Nevertheless, the relative shifts of the Au 5d in the RAuSn series are quantitatively well reproduced, with the Au 5d of the hexagonal compounds ($R=\text{Ce, Gd, and Er}$) at consistently lower binding energies as compared to those of the cubic compounds ($R=\text{Sc and Lu}$). This could well be due to the stronger electric field of the R^{3+} cations with the shorter $R\text{--Au}$ bond lengths in the closely packed fcc structure of the latter. The same can be observed for the Au 4f core levels which are shifted by the same amount as the Au 5d levels. Figure 3 displays the experimental Au 4f core levels together with the results from the LDA+ U calculations. As a reference we have also included data from Au metal. We can clearly see that the relative shifts between the Au metal, the hexagonal, and the cubic compounds are well reproduced by the calculations.

To capture the energy positions of the rare-earth 4f orbitals, the Hubbard U correction has to be included in the band structure calculations to account for correlation effects that occur for these atomiclike orbitals. The applied U values are 5 eV for the Ce 4f and 7 eV for the 4f of Gd, Er, and Lu. The implementation of U has the effect of shifting the occupied R 4f levels to higher binding energies by $\frac{1}{2}U$, and in this

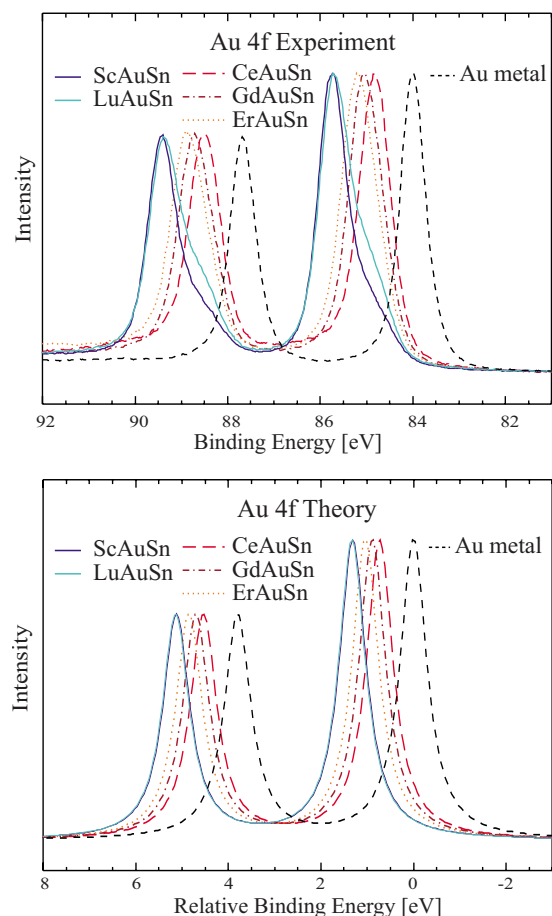


FIG. 3. (Color online) Experimental (top panel) and calculated (bottom panel) Au 4f core-level photoemission spectra of Au metal, the hexagonal compounds CeAuSn, GdAuSn, and ErAuSn, as well as the cubic compounds ScAuSn and LuAuSn.

way the energy positions of the 4f in the LDA+ U calculations can be well tuned to the experimental values, see Fig. 2. However, in the case of the partially filled 4f shells of the Gd and, in particular, the Er, the line shape of the spectra is determined by the multiplet structure in the photoemission final states and these cannot be described by a one-electron theory.

The LDA/LDA+ U is highly adequate to treat the band structure of spatially extended states. In the present case, these are the rare-earth 6s, 6p, and 5d and the Au and Sn s and p bands. Their densities of states are lumped together and denoted as “rest” in the calculated partial density of states in Fig. 2. They are spread from the Fermi level up to 10 eV binding energy and can be seen in the experimental spectra most clearly as a broad hump between the Fermi level and 3 eV binding energy and, for ScAuSn and CeAuSn, at about 9 eV as well. The weight of these broadbands relative to those of the Au 5d and the rare-earth 4f levels is smaller in the experiment than in the calculations, in accordance with the tabulated photoionization cross sections.²⁵

A close-up of the experimental photoemission spectra in the region near the Fermi level is shown in the top panel of Fig. 4. One can clearly observe that the spectral weight of all

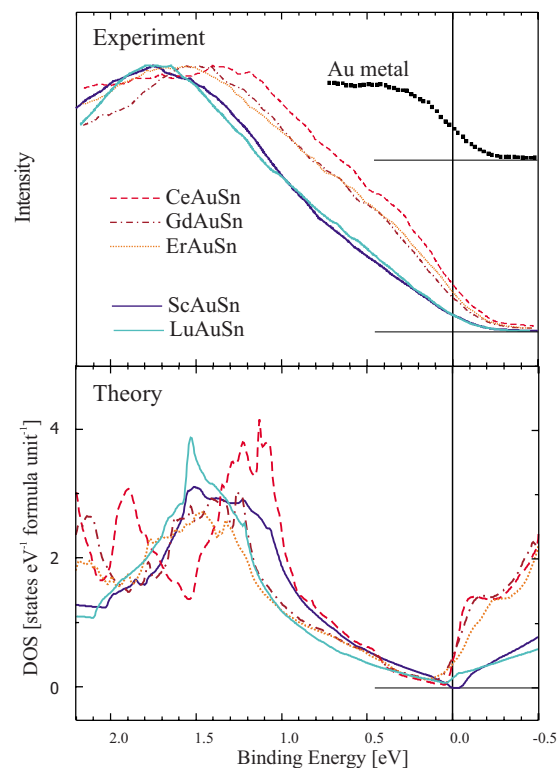


FIG. 4. (Color online) Close-up of the experimental photoemission spectra (top panel) in the vicinity of the Fermi level together with the calculated density of states (bottom panel).

compounds becomes smaller and almost vanishes upon approaching the Fermi level. This is in contrast to the spectrum of a reference Au sample (also included in Fig. 4) which clearly shows a distinct cut off at the Fermi edge. Interestingly, the LDA/LDA+ U calculations also show extremely low density of states near the Fermi level, see the bottom panel of Fig. 4. In fact, the calculations even find a tiny band gap of less than 0.2 eV for ScAuSn and almost a gap for LuAuSn.

The formation of the band gap in the cubic compounds such as ScAuSn was already found by previous band structure calculations.^{19,20} $RAuSn$ can be written as R^{3+} and $(AuSn)^{3-}$, the latter forming a zinc blend structure in which both Au and Sn are tetrahedrally coordinated by each other. Disregarding the ten Au 5d electrons which can be considered as almost core-like states, each $(AuSn)^{3-}$ unit has eight valence electrons leading to completely filled bonding sp bands while the antibonding counterpart is unfilled, provided that the bonding-antibonding splitting is sufficiently large and that the bandwidth is not large enough to close the gap. Since the Au-Sn distance is shorter in ScAuSn (2.78 Å) than in LuAuSn (2.84 Å), one would expect the bonding-antibonding splitting to be larger in ScAuSn than in LuAuSn. As a result, the band gap is manifest in ScAuSn but not quite in LuAuSn.

To investigate to what extent the physical properties of these cubic and hexagonal intermetallics are influenced by the small or vanishing density of states at the Fermi level, we measured their resistivity as a function of temperature. The

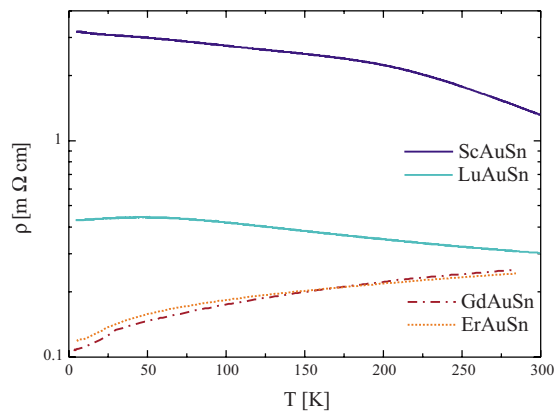


FIG. 5. (Color online) Temperature dependence of the resistivity of cubic ScAuSn and LuAuSn and hexagonal GdAuSn and ErAuSn.

results are shown in Fig. 5. The resistivity decreases weakly with increasing temperature for ScAuSn and, to a lesser degree, also for LuAuSn, indicating a semiconducting or near-semiconducting character for these cubic compounds, in agreement with the finding that there is a gap or almost a gap

in the electronic structure. For the hexagonal GdAuSn and ErAuSn, we observe that the resistivities are an order of magnitude lower and increase with temperature, indicating that indeed they are more metalliclike.

To conclude, we have determined the electronic structure of the cubic intermetallic compounds ScAuSn and LuAuSn, as well as the hexagonal CeAuSn, GdAuSn, and ErAuSn, using x-ray photoelectron spectroscopy and band structure calculations. The rare-earth $4f$ and Au $5d$ have well identified spectral features far away from the Fermi level. The spectral weight in the vicinity of the Fermi level, of mainly Au/Sn sp and rare-earth spd characters, is found to be vanishingly small. For the cubic compounds, we even find that a band gap can be opened in the electronic structure, in agreement with the semiconducting or almost semiconducting temperature dependence of the resistivity.

We acknowledge Lucie Hamdan for her skillful technical assistance. We thank the Degussa-Hüls AG for the generous gift of noble metals. This work was supported by the Deutsche Forschungsgemeinschaft through the priority programme SPP 1166 “Lanthanoid-spezifische Funktionalitäten in Molekül und Material.”

- ¹C. Peter Sebastian, H. Eckert, S. Rayaprol, R.-D. Hoffmann, and R. Pöttgen, *Solid State Sci.* **8**, 560 (2006), and references therein.
- ²G. Wenski and A. Mewis, *Z. Kristallogr.* **176**, 125 (1986).
- ³R.-D. Hoffmann and R. Pöttgen, *Z. Kristallogr.* **216**, 127 (2001).
- ⁴H. Nowotny and W. Sibert, *Z. Metallkd.* **33**, 391 (1941).
- ⁵A. E. Dwight, in *Proceedings of the 12th Rare Earth Conference*, edited by C. E. Lundin (Denver Research Institute, Denver, 1976), p. 480.
- ⁶S. Baran, M. Hofmann, J. Leciejewicz, M. Ślaski, A. Szytuła, and A. Zygmunt, *J. Phys.: Condens. Matter* **9**, 9053 (1997).
- ⁷S. Baran, P. Hofmann, N. Stüsser, A. Szytuła, P. Smeibidl, and S. Kausche, *J. Magn. Magn. Mater.* **231**, 94 (2001).
- ⁸K. Łątka, W. Chajec, R. Kmiec, A. W. Pacyna, and J. Gurgul, *J. Alloys Compd.* **383**, 265 (2004).
- ⁹H. Oesterreicher, *J. Less-Common Met.* **55**, 131 (1977).
- ¹⁰S. Baran, J. Leciejewicz, M. Ślaski, P. Hofmann, and A. Szytuła, *J. Alloys Compd.* **275-277**, 541 (1998).
- ¹¹M. Lenkewitz, S. Corsepius, and G. R. Stewart, *J. Alloys Compd.* **241**, 121 (1996).
- ¹²D. T. Adroja, B. D. Rainford, and A. J. Neville, *J. Phys.: Condens. Matter* **9**, L391 (1997).
- ¹³K. Łątka, W. Chajec, R. Kmiec, and A. W. Pacyna, *J. Magn. Magn. Mater.* **224**, 241 (2001).
- ¹⁴F. Casper, V. Ksenofontov, H. C. Kandpal, S. Reiman, T. Shishido, M. Takahashi, M. Takeda, and C. Felser, *Z. Anorg. Allg. Chem.* **632**, 1273 (2006).
- ¹⁵A. Szytuła, A. Jezierski, B. Penc, and D. Fus, *J. Magn. Magn. Mater.* **222**, 47 (2000).
- ¹⁶A. Szytuła, D. Fus, B. Penc, and A. Jezierski, *J. Alloys Compd.* **317-318**, 340 (2001).
- ¹⁷A. Szytuła, A. Jezierski, B. Penc, A. Winiarski, A. Leithe-Jasper, and D. Kaczorowski, *J. Alloys Compd.* **360**, 41 (2003).
- ¹⁸V. I. Anisimov, I. V. Solovyev, M. A. Korotin, M. T. Czyżyk, and G. A. Sawatzky, *Phys. Rev. B* **48**, 16929 (1993).
- ¹⁹H. C. Kandpal, C. Felser, and R. Seshadri, *J. Phys. D* **39**, 776 (2006).
- ²⁰J. Köhler, S. Deng, C. Lee, and M.-H. Whangbo, *Inorg. Chem.* **46**, 1957 (2007).
- ²¹J. Gegner, T. C. Koethe, H. Wu, H. Hartmann, T. Lorenz, T. Fickenscher, R. Pöttgen, and L. H. Tjeng, *Phys. Rev. B* **74**, 073102 (2006).
- ²²M. Campagna, G. K. Wertheim, and Y. Baer, in *Topics in Applied Physics*, edited by L. Ley and M. Cardona (Springer-Verlag, Berlin, 1979), Vol. 27.
- ²³J. K. Lang, Y. Baer, and P. A. Cox, *J. Phys. F: Met. Phys.* **11**, 121 (1981).
- ²⁴F. Gerken, *J. Phys. F: Met. Phys.* **13**, 703 (1983).
- ²⁵J. J. Yeh and I. Lindau, *At. Data Nucl. Data Tables* **32**, 1 (1985).
- ²⁶P. Blaha, K. Schwarz, G. Madsen, D. Kvasnicka, and J. Luitz, <http://www.wien2k.at>
- ²⁷D. Niepmann, R. Pöttgen, K. M. Poduska, F. J. DiSalvo, H. Trill, and B. D. Mosel, *Z. Naturforsch., B: Chem. Sci.* **56**, 1 (2001).